Drivetrain load effects in a 5-MW bottom-fixed wind turbine under blade-pitch fault condition and emergency shutdown

2016 J. Phys.: Conf. Ser. 753 112011

(http://iopscience.iop.org/1742-6596/753/11/112011)

Drivetrain load effects in a 5-MW bottom-fixed wind turbine under blade-pitch fault condition and emergency shutdown

Amir Rasekhi Nejad, Zhiyu Jiang, Zhen Gao, Torgeir Moan

Centre for Ships and Ocean Structures (CeSOS) & Centre for Autonomous Marine Operations and Systems (AMOS), Department of Marine Technology, Norwegian University of Science and Technology (NTNU)

E-mail: Amir.Nejad@ntnu.no

Abstract. In this paper, the effect of the blade-pitch fault and emergency shutdown on drivetrain responses in a 5-MW bottom-fixed wind turbine are investigated. A 5-MW reference gearbox with 4-point support is employed and the decoupled analysis approach is used for the load effect analysis. The effect of this fault event is then investigated for all bearings and gears inside the gearbox as well as main bearings. The results show that the blade-pitch fault creates significant axial forces on main bearings which increases the nontorque force entering the gearbox. Due to the emergency shutdown, the rotor torque reversal occurs which causes force reversals in gears. The main bearings are more affected than gears and bearings inside the gearbox in this fault condition and emergency shutdown, but first-stage bearings may also be considerably affected. It is therefore recommended to conduct a thorough inspection of main bearings and first stage bearings in case of such blade-pitch fault condition and emergency shutdown.

1. Introduction

Wind energy development has been recently ahead of any other renewable technologies [1]. By the end of 2014, the total installed wind turbine capacity around the world was estimated to be 370 GW and more than 20% of the electricity demand in Denmark, Portugal, Nicaragua and Spain was supplied by the wind power [1]. There have also been extensive works on developing state-of-the-art design codes and best practices to design reliable and cost effective wind turbines. For design of onshore or offshore wind turbines, a set of load cases has been specified by the International Electrotechnical Commission (IEC) [2] to address extreme as well as fatigue life of the turbine components. These load cases cover various design situations such as normal power production, fault condition, and extreme environment. Many recent works have been devoted to the structural analysis of wind turbines in normal operational condition (e.g. [3, 4, 5, 6]). Similarly, there have been works on the drivetrain in operational condition (e.g. [7, 8, 9, 10, 11, 12]).

In recent years, load cases that arise from certain fault conditions have received attention. These events are rare, but may change the external loads and cause large structural and motion responses [13, 14]. For an operating turbine, if shutdown takes place in the event of faults, the shutdown procedure plays an important role in the extreme response [15]. However, most existing

publications on this topic applied aeroelastic tools using simplified drivetrain models, thus the effect on the drivetrain components are not captured. It remains unclear the consequence of these events on the internal response of drivetrain. Are the fault cases key to the drivetrain design? Which components in drivetrain are more vulnerable in case of faults? Is any drivetrain inspection needed after the fault occurred? This study aims to address these questions for the blade-pitch fault condition followed by an emergency shutdown.

2. Wind Turbine and Drivetrain Model

The 5-MW reference gearbox [16] installed on the NREL 5-MW wind turbine [17] was used in this study. This turbine is a pitch-regulated, variable-speed, three-bladed upwind wind turbine - see Table 1.

Table 1: Wind turbine specifications [17, 18].

Parameter	Value
Type	Upwind/3 blades
Cut-in, rated and cut-out wind speed (m/s)	3, 11.4, 25
Hub height (m)	87.6
Rotor diameter (m)	126
Hub diameter (m)	3
Rotor mass (×1,000 kg)	110
Nacelle mass (×1,000 kg)	240
Hub mass (×1,000 kg)	56.8

This 5-MW reference gearbox was developed by Nejad et al. [16] for offshore wind turbines. It follows the most conventional design types of those used in wind turbines and consists of three stages, two planetary and one parallel stage gears. Table 2 shows the general specifications of this gearbox. Figure 1 shows the gearbox and drivetrain layout. The gearbox topology is also shown in Figure 2. The gearbox was designed with a 4-point support with two main bearings to reduce nontorque loads entering the gearbox [19]. The wind turbine gearbox failure data is also shown that the average annual failure rate of 4-point support ($\sim$ 0.8% per year) is by far less than the 3-point support configuration ($\sim$ 5.9% per year) [20]. In addition the main bearing failure rate is less in 4-point support than in the 3-point [20].

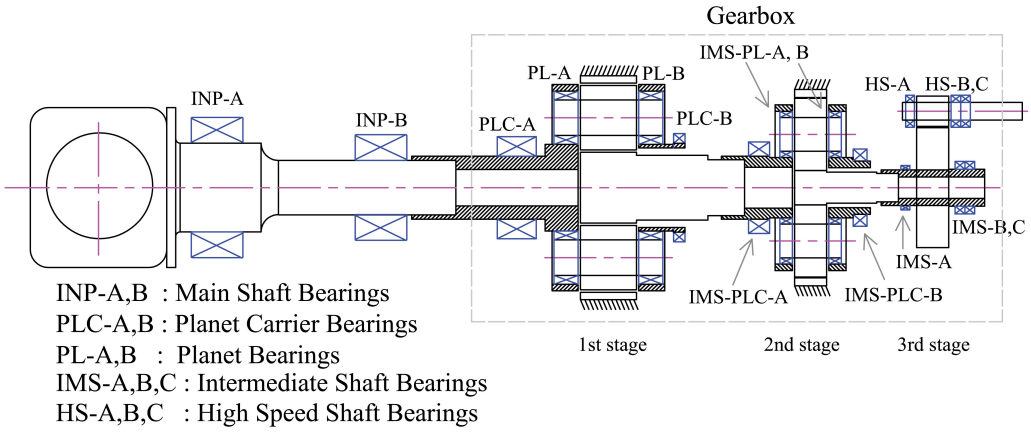

Figure 1: 5-MW reference drivetrain layout [16].

Table 2: 5-MW reference gearbox specification [16].

Parameter	Value
Type	2 Planetary + 1 Parallel
1st stage ratio	1:3.947
2nd stage ratio	1:6.167
3rd stage ratio	1:3.958
Total ratio	1:96.354
Designed power (kW)	5000
Rated input shaft speed (rpm)	12.1
Rated generator shaft speed (rpm)	1165.9
Rated input shaft torque (kN.m)	3946
Rated generator shaft torque (kN.m)	40.953
Total dry mass (×1000 kg)	53
Service life (year)	20

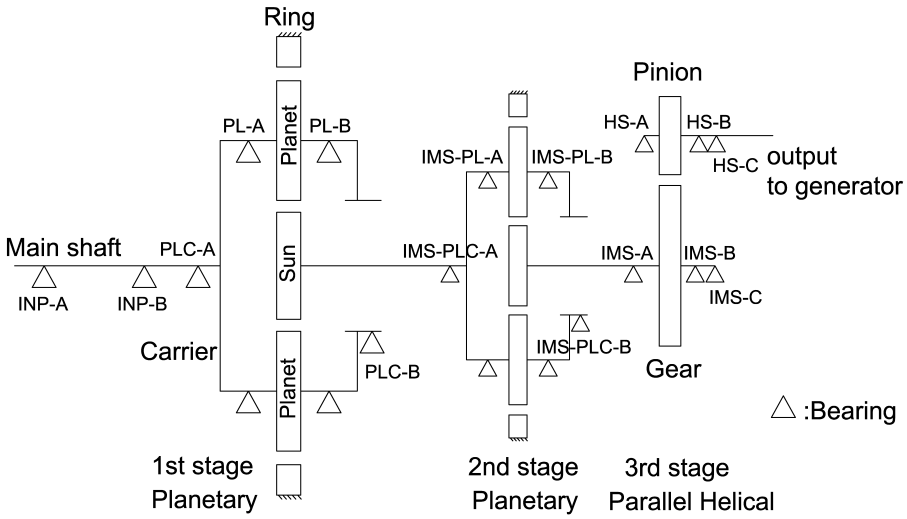

Figure 2: 5-MW reference gearbox topology [16].

3. Methodology

A two-step decoupled approach was employed in this study [7, 19]. First, aeroelastic simulations were performed in the time domain to obtain the rotor torque and the nontorque loading on the main shaft. These loads are input to a detailed gearbox model for multibody simulations (MBS).

The excitations of wind turbine gearboxes are classified into two general groups: external and internal. The external excitations from wind and waves are in the low frequency range, often less than 2 Hz. Moreover, the wave- and wind-induced tower motions may appear in the power spectra of the gearbox responses, and are also classified as external excitations. The internal excitations consist of gear mesh frequency and its harmonics and side bands which are normally in the high frequency range, above 20 Hz. Therefore, in order to capture the internal resonances, simulations with very small time steps (e.g. 0.005 s) are required, while simulations with 0.1 s can often capture possible responses to external excitations.

The different simulation frequency requirements as well as the computational requirements for complex gearbox models encourage using a decoupled analysis approach. Figure 3 presents a schematic procedure of the decoupled analysis approach for wind turbine gearbox analysis.

The HAWC2 code was used for the aeroelastic simulations [21]. The control actions, as

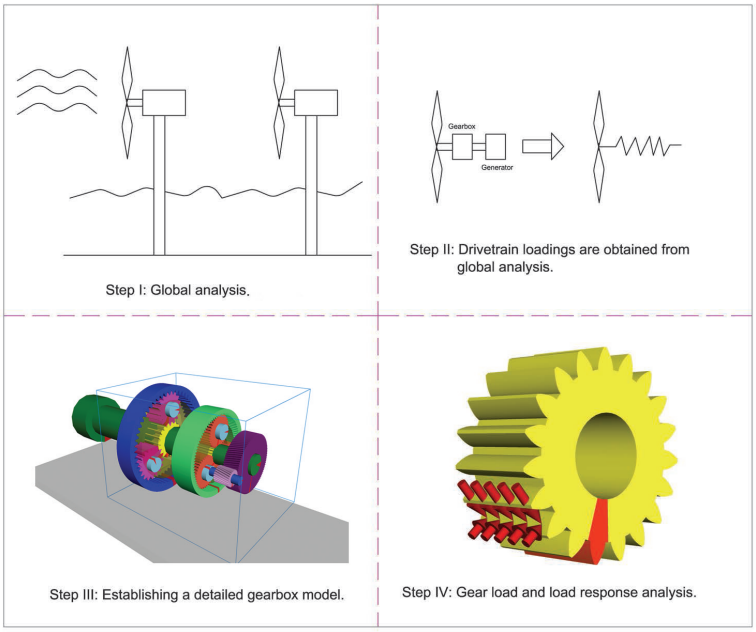

Figure 3: Drivetrain decoupled analysis method [7].

well as external load effects can be achieved through external dynamic link libraries (DLL's). The blade-pitch and generator torque control during normal operation are based on the NREL-developed operational controller. Under the specified fault conditions, the operational controller is superseded by user-defined subroutines compiled in the computing language, Delphi. These control actions are handled by DLL's. The time-domain simulations were conducted using Newmark-beta integration.

Figure 4 shows the MBS model of the 5-MW reference gerabox developed in SIMPACK [22]. In the MBS analysis, bearings are modelled as force elements and their force-deflection relations. Gears are modelled with compliance at tooth including detailed tooth properties [16]. The generator should also be modelled. The generator model depends on the choice of the generator. Synchronous generators act as power-dependent torsional springs, whereas asynchronous or induction generators are modelled by dampers in operating conditions or free-free lumped masses [23]. In this paper an asynchronous generator was considered and modelled.

Earlier works on wind turbine gearboxes based on the decoupled method include, for instance Xing et al. [24], Dong et al. [25], Jiang et al. [26] and Nejad et al. [7].

3.1. Load Cases

Table 3 lists the load cases (LC's) covered by this study. In the table, Uw refers to the 10-min mean wind speed at hub height and Pr is the pitch rate during shutdown. LC1 is the fault case relevant to design load case (DLC) 2.2 of the design standards [2, 27]. Before the specified time, about 395 s. , the turbine is under normal operation. Because of the actuator fault, blade 2 is seized and has a fixed pitch angle. It is assumed that the control system detects the fault after a short time delay (0.1 s), and reacts by pitching to feather the remaining two blades at the maximum pitch rate of 8 deg/s and disconnecting the generator. The results for the wind speed of 14 m/s are presented in this paper.

The turbulence model was used to include the effects of varying wind speed, shear, and direction. For this study the normal turbulence model (NTM) of class A was used to calculate the turbulence intensity.

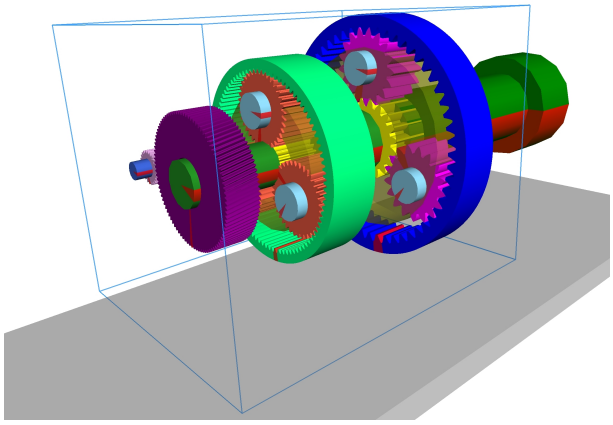

Figure 4: MBS model of the 5-MW reference gearbox.

Table 3: Load cases.

LC	Description	Uw (m/s)	Wind model	Pr (deg/s)
LC0	Normal operation	14	NTM	-
LC1	Blade-pitch fault and emergency shutdown	14	NTM	8

4. Results

The load effects of bearings and gears for normal operation (LC0) and the blade-pitch fault with emergency shutdown (LC1) are compared and presented in this section.

Two important variables, rotor torque and bending moment on the main shaft, obtained from the global analysis are first compared - see Figure 5. A considerable torque reversal and a sudden peak in the bending moment are observed for LC1 near 400 s.

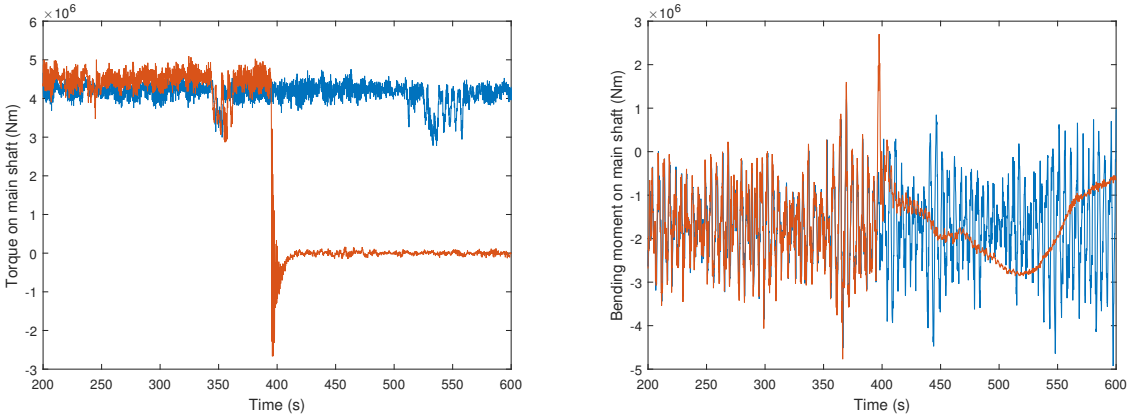

(a) Torque on the main shaft.

(b) Bending moment on the main shaft.

Figure 5: Input loadings on the main shaft (LC0: blue, LC1: red).

The rotor torque reversal causes gear mesh force reversal and possible tooth rattle - see Figure 6a - while the large bending moment causes large radial force on the first main bearing (INP-A) as shown in Figure 6b. INP-A is the bearing which holds the most of the radial load on the main shaft. The impact due to the fault and shutdown is about 1.5 times of the mean value for

this bearing. The gear mesh force reversal is seen throughout the gearbox in the 2nd and the 3rd stages - see Figure 7.

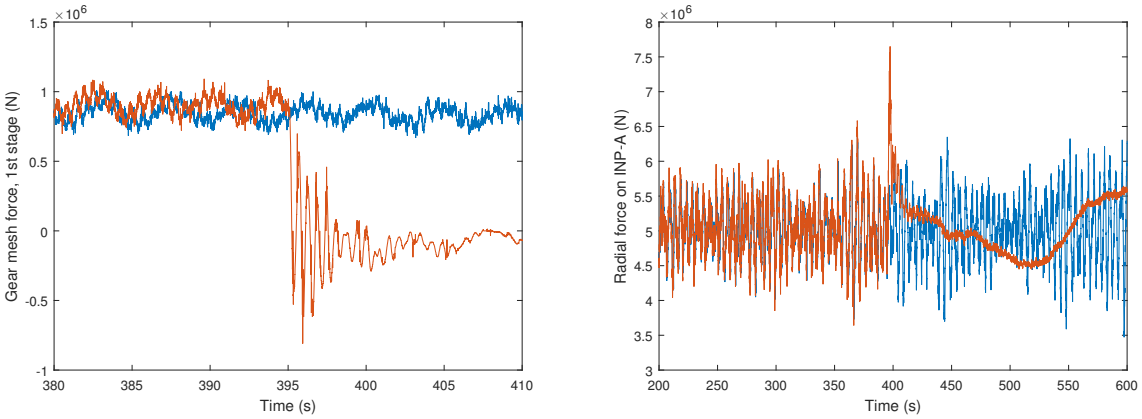

(a) Gear mesh force, 1st stage. (b) Radial force on INP-A.

Figure 6: Radial force on INP-A (see Figure 1) & gear mesh force (LC0: blue, LC1: red).

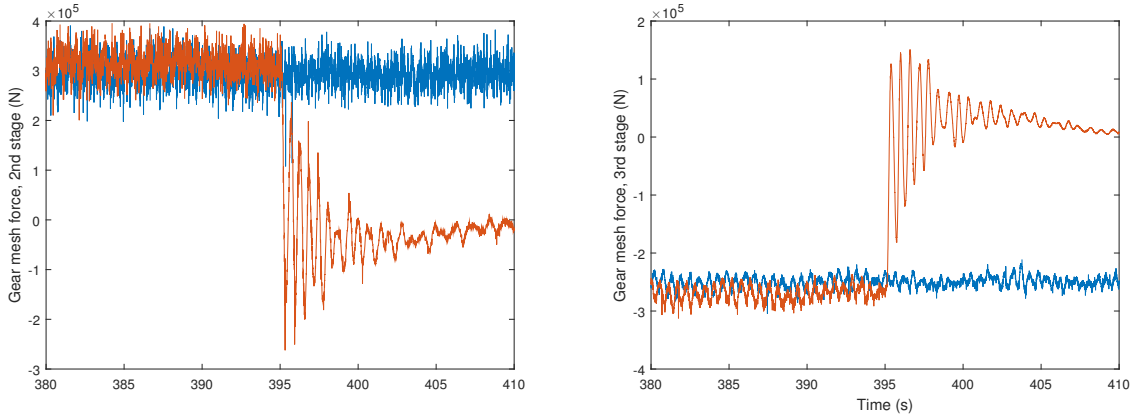

(a) Gear mesh force, 2nd stage. (b) Gear mesh force, 3rd stage.

Figure 7: Gear mesh force in 2nd and 3rd stages (LC0: blue, LC1: red).

The second main bearing (INP-B) is the one that carries the axial force. As it is shown in Figure 8a, the blade-pitch fault and shutdown creates a large axial force on this bearing, while the radial force is not significant - see Figure 8b. The axial force changes are due to changes in thrust force caused by the emergency shutdown following the fault. This also affects bearings inside the gearbox, in particular the carrier bearings at the first stage like PLC-B, but less severe than INP-B.

The simulation results also indicate that the planet bearings are less effected than carrier bearings by this fault and shutdown case. Moreover, the large bending moment causes deformation along the main shaft and on the first-stage carrier.

5. Discussions and Concluding Remarks

The blade-pitch fault followed by an emergency shutdown and their effects on the drivetrain was studied in this paper. The global responses were estimated by an aero-servo-elastic code,

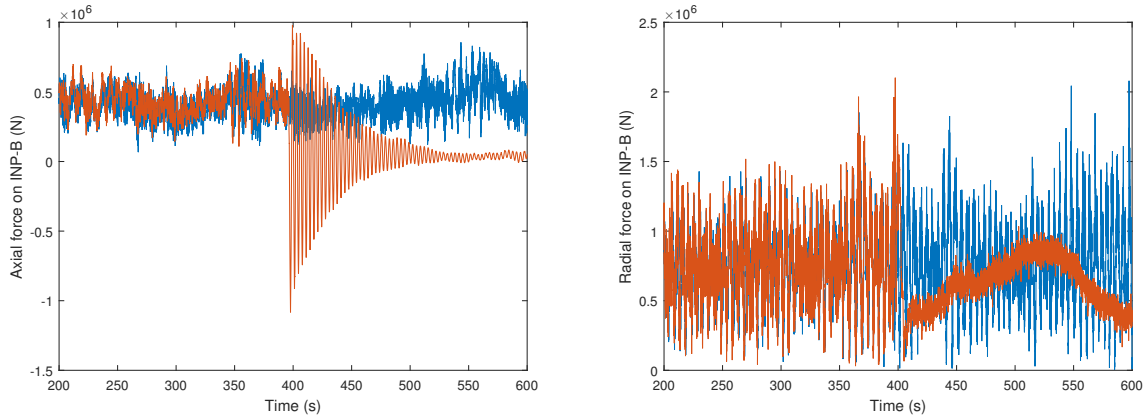

(a) Axial force. (b) Radial force.

Figure 8: Axial and radial forces on INP-B (LC0: blue, LC1: red).

HAWC2, and were applied on a detailed MBS model in SIMPACK. The simulation was carried out for above rated wind speed of 14 m/s and load effects of bearings and gears for both fault (LC1) and nonfault (LC0) cases were compared.

The results show that the blade-pitch fault creates a considerable axial force on the main bearing which goes through the gearbox and affects other bearings, in particular the carrier bearings in the first stage. This increases significantly the nontorque loads entering the gearbox. When the fault is followed by an emergency shutdown, the torque reversal occurs which may cause gear rattle in all stages.

Moreover, it is seen that the main bearings (INP-A and INP-B) are the most effected components due to this fault and shutdown case. They are followed by the carrier bearings in the first stage. The gears and bearings inside the gearbox - for example the planet bearings - are less effected than the main bearings due to the fault and the emergency shutdown.

The question may raise here is whether this fault case and emergency shutdown are key to the drivetrain design. According to IEC 61400-1 [2] the ultimate limit analysis should be carried out for emergency shutdown and fault cases (DLC 2 and 5). An earlier study [28] shows that the extreme long-term torque in normal operation can reach to 1.82 times of the rated torque. From Figure 5, it is evident that the torque maximum value in this fault case is less than the one obtained from the long-term extreme value analysis in the normal operation. Therefore, with respect to the torque, this fault case is not a key design driver.

About bearings, estimation of the extreme long-term radial and axial forces in normal operation requires further study, but it should be noted that often bearing life is governed by fatigue life of its components. From the Lundberg-Palmgren hypothesis, the bearing life is expressed by [29, 30]:

$$L = (\frac{C}{P})^a \tag{1}$$

in which L is the bearing basic life defined as the number of cycles that 90% of an identical group of bearings achieve, under a certain test conditions, before the fatigue damage appears. C is the basic load rating and is constant for a given bearing. The parameter $a = \frac{10}{3}$ for roller bearings such as INP-A and INP-B. P is the dynamic equivalent radial load calculated from:

$$P = XF_r + YF_a \tag{2}$$

where F_a and F_r are the axial and radial loads on the bearing respectively and X and Y are constant factors obtained from the bearing manufacturer [29].

For INP-A, Equation 2 is read as $P = F_r$ and for INP-B as $P = F_r + 2.4F_a$. The 1.5 times increase of P, as observed for INP-A, can reduce its fatigue life in the order of $1.5^a = 3.86$ times with respect to the normal operation. This indicates that under this fault case, there can be a considerable accumulation of fatigue damage. This is more severe for INP-B as the axial force on this bearing is amplified by a factor of 2.4.

Consequently, this fault scenario and emergency shutdown can be a design driver for bearings, in particular for main bearings. In designing a drivetrain, main bearings should be designed for such extreme loads, and depends on the probability of the fault occurrence, their remaining fatigue life should be evaluated based on the site specific environmental conditions. It is also recommended to carry out an inspection after the fault event to examine the rollers and races for possible cracks. The inspection should focus on main bearings and first stage carrier bearings.

Acknowledgements
The authors wish to acknowledge the financial support from Research Council of Norway through Center for Ships and Ocean Structures (CeSOS) and partially from Centre for Autonomous Marine Operations and Systems (AMOS-Project number 223254) at Department of Marine Technology, Norwegian University of Science and Technology (NTNU).

References

[1] REN21. Renewables, global status report 2015, 2015.
[2] IEC 61400-1. Wind turbines, part 1: Design requirements, 2005.
[3] Bachynski EE. and Moan T. Design considerations for tension leg platform wind turbines. *Marine Structures*, 29(1):89–114, 2012.
[4] Karimirad M. and Moan T. A simplified method for coupled analysis of floating offshore wind turbines. *Marine Structures*, 27(1):45–63, 2012.
[5] Kim T., Petersen M.M., and Larsen T.J. A comparison study of the two-bladed partial pitch turbine during normal operation and an extreme gust conditions. In *Journal of Physics: Conference Series*, volume 524, page 012065. IOP Publishing, 2014.
[6] Lefebvre S. and Collu M. Preliminary design of a floating support structure for a 5 {MW} offshore wind turbine. *Ocean Engineering*, 40:15 – 26, 2012.
[7] Nejad A.R., Gao Z., and Moan T. On long-term fatigue damage and reliability analysis of gears under wind loads in offshore wind turbine drivetrains. *International Journal of Fatigue*, 61:116–128, 2014.
[8] Xing Y. and Moan T. Multibody modelling and analysis of a planet carrier in a wind turbine gearbox. *Wind Energy*, 16(7):1067–1089, 2013.
[9] Nejad A.R., Odgaard P.F., Gao Z., and Moan T. A prognostic method for fault detection in wind turbine drivetrains. *Engineering Failure Analysis*, 42:324 – 336, 2014.
[10] Nejad A.R., Xing Y., Guo Y., Keller J., Gao Z., and Moan T. Effect of floating sun gear in wind turbine planetary gearbox with geometrical imperfections. *Wind Energy*, 18(12):2105–2120, 2015.
[11] Gallego-Calderon J. and Natarajan A. Assessment of wind turbine drive-train fatigue loads under torsional excitation. *Engineering Structures*, 103:189–202, 2015.
[12] Guo Y., Keller J., and LaCava W. Planetary gear load sharing of wind turbine drivetrains subjected to non-torque loads. *Wind Energy*, 18(4):757–768, 2015.
[13] Jonkman J.M. and Buhl M.L. *Loads analysis of a floating offshore wind turbine using fully coupled simulation*. National Renewable Energy Laboratory, Technical report NREL/EL-500-41714, 2007.
[14] Jiang Z., Karimirad M., and Moan T. Dynamic response analysis of wind turbines under blade pitch system fault, grid loss, and shutdown events. *Wind Energy*, 17(9):1385–1409, 2014.
[15] Jiang Z., Moan T., and Gao Z. A comparative study of shutdown procedures on the dynamic responses of wind turbines. *Journal of Offshore Mechanics and Arctic Engineering*, 137(1):011904, 2015.
[16] Nejad A.R., Guo Y., Gao Z., and Moan T. Development of a 5 MW reference gearbox for offshore wind turbines. *Wind Energy*, 19(6):1089 – 1106, 2016.
[17] Jonkman J., Butterfield S., Musial W., and Scott G. Definition of a 5-MW reference wind turbine for offshore system development. Technical Report NREL/TP-500-38060, US National Renewable Energy Laboratory (NREL), 2009.
[18] Jonkman J. *Definition of the Floating System for Phase IV of OC3*. National Renewable Energy Laboratory, 2010.

[19] Nejad A.R., Bachynski EE., Kvittem M.I., Luan C., Gao Z., and Moan T. Stochastic Dynamic Load Effect and Fatigue Damage Analysis of Drivetrains in Land-based and TLP, Spar and Semi-Submersible Floating Wind Turbines. *Marine Structures*, 42:137–153, 2015.
[20] Berger B. Major component failure data & trends. Operations and Maintenance Summit Proceedings, 24-25 Feb. 2016, Toronto, Canada, 2016.
[21] Hawc2. Aero-servo-elastic calculation code for horizontal axis wind turbine, Risoe centre, Denmark Technical University (DTU); Denmark. `www.hawc2.dk/`. [Online; accessed 10-April-2014].
[22] SIMPACK. Multi body system software. `www.simpack.de/`. [Online; accessed 03-April-2014].
[23] Hau E. *Wind Turbines Fundamentals, Technologies, Application, Economics*. Springer, 2nd edition, 2006.
[24] Xing Y., Karimirad M., and Moan T. Modelling and analysis of floating spar-type wind turbine drivetrain. *Wind Energy*, 17:565–587, 2014.
[25] Dong W., Xing Y., Moan T., and Gao Z. Time domain-based gear contact fatigue analysis of a wind turbine drivetrain under dynamic conditions. *International Journal of Fatigue*, 48:133–146, 2013.
[26] Jiang Z., Xing Y., Guo Y., Moan T., and Gao Z. Long-term contact fatigue analysis of a planetary bearing in a land-based wind turbine drivetrain. *Wind Energy*, 18(4):591–611, 2015.
[27] Germanischer Lloyd Industrial Services GmbH, guideline for the certification of wind turbines, 2010.
[28] Nejad A.R., Gao Z., and Moan T. Long-term analysis of gear loads in fixed offshore wind turbines considering ultimate operational loadings. *Energy Procedia*, 35:187–197, 2013.
[29] ISO 281. Rolling bearings - dynamic load ratings and rating life, 2007.
[30] IEC 61400-4. Wind turbines, part 4: Standard for design and specification of gearboxes, 2012.